



Detection of fractures in resistive image logs using Hough Transform

Ciro Moraes & Abel Carrasquilla, UENF/LENP, Macaé - RJ

Copyright 2017, SBGf - Sociedade Brasileira de Geofísica

This paper was prepared for presentation during the 15th International Congress of the Brazilian Geophysical Society held in Rio de Janeiro, Brazil, 31 July to 3 August, 2017.

Contents of this paper were reviewed by the Technical Committee of the 15th International Congress of the Brazilian Geophysical Society and do not necessarily represent any position of the SBGf, its officers or members. Electronic reproduction or storage of any part of this paper for commercial purposes without the written consent of the Brazilian Geophysical Society is prohibited.

Abstract

The extraction of hydrocarbons requires the determination of the properties of a reservoir efficiently, and, as a consequence, it is necessary to continuously improve the technologies capable of executing this task. The resistive, density or acoustic reflectivity image logs have, at present, a fundamental role in the characterization of reservoirs, being the resistive ones represents an evolution of dipmeter tools of high resolution (micro electrodes) and laterolog (macro electrodes). This work validated a methodology for the characterization of reservoir rock fractures in resistive images. For this, a program was developed that used the Hough Transform to analyze fractures in logs in a semi – automatic way. In order to validate the methodology, the results obtained were compared with those of the literature and with the analysis done by a geologist, and it can be said that the results were satisfactory for the analyzed data, when determining the same number of fractures in both cases.

Introduction

The demand for hydrocarbons makes it necessary to develop techniques that help in the determination of the geological characteristics of the reservoirs, such as structural, sedimentary and stratigraphic. In this sense, the image logs provide high resolution data, increasing the capacity of understanding these characteristics and attributes of the reservoir rock inside a well. To do so, these logs use physical properties such as electrical resistivity, density and acoustic impedance generate images of the well wall (Ellis & Singer, 2007).

The Hough Transform (TH) is a mathematical technique that performs the detection of geometric shapes in digital images, which was elaborated by Paul Hough and patented by IBM in 1962 (Hough, 1962). TH is a technique that can be used to isolate pre-determined characteristic formats within a binarized image (Prensky, 1999). Due to the need to specify the desired format parametrically, TH is commonly used for the detection of regular curves such as lines, circles and ellipses (Glossop et al., 1999). The major advantage of TH is that it is tolerant to discontinuities at the edges of the image sought, and also, it is relatively immune to noise (Jain, 1989). To understand the TH, consider the points (x_i, y_i) and the general equation of the line in the form:

$$y_i = ax_i + b, \quad (1)$$

where infinite lines passing through (x_i, y_i) , but all satisfy Equation 1 for different values of a and b . This equation can be written like this (Albinhassan & Marfurt, 2003):

$$b = -ax_i + y_i, \quad (2)$$

and we consider the plane ab , also called the parameter space, this leads us to the equation of a single line given a fixed pair (x_i, y_i) . In addition, a second point (x_j, y_j) also has a line in the parameter space associated with it, and this line intersects the line associated with (x_i, y_i) at (a_0, b_0) , where a_0 is the slope of straight and b_0 is the point of intersection with the y -axis of the line containing (x_i, y_i) and (x_j, y_j) in the xy plane (Thapa et al., 1997). Figure 1a illustrates these concepts presented (Gonzalez & Woods, 2000).

The computational advantage obtained with the use of TH comes from the subdivision of the space of the parameters in the so-called accumulator cells, as shown in Figure 1b, where (a_{max}, a_{min}) and (b_{max}, b_{min}) are the expected domains of slope and point of intersection. The cell in the coordinates (i, j) with value $A(i, j)$ of the accumulator corresponds to the square associated with the coordinates (a_i, b_j) . Originally these cells are initialized to zero. Then, for each point (x_k, y_k) in the plane of the image, the parameter a is varied within each sub-division value of the axis a and the corresponding b is calculated using Equation 2. The resulting b values are then rounded to the nearest allowed value of axis b . If the choice of a given a results in a solution b , $A(p, q) = A(p, q) + 1$ is made. At the end of this procedure, a value M in $A(i, j)$ corresponds to M points in the xy plane that lie on the line represented by Equation 1. A problem found in this equation for line representation is that both the slope and the point Intersection approaches the infinite as the line becomes vertical. Thus, Duda and Hart (1992) used polar coordinates to represent a line. Then, the lines could be completely parameterized using the angle (of its normal and the algebraic distance of the origin of the image). The parameterized equation of the line is then given by:

$$\rho = x \cos \theta + y \sin \theta. \quad (3)$$

Figure 1c shows the relationship of the line with the factors used in the parameterization. Using this technique, every point (x, y) in the line will satisfy Equation 3. After the transformation, Duda and Hart (1992) summarized the properties of TH in polar coordinates: a) a point in the plane of the image corresponds to a sinusoid in the plane of the parameters; B) a point in the plane of the parameters corresponds to a straight line in the plane of the image; C) points in the same straight line in the plane of the image corresponds to curves passing through a common point in the plane of the parameters; D) points on the same curve in the plane of the parameters correspond to lines crossing the same point in the plane of the image (Figure 2).

Method

The steps followed in the methodology consisted, initially, in a preprocessing of the resistive images. Next, the images were analyzed line by line, resulting in the continuation of the transformed plane. Finally, the histograms were generated and the cutoff points were defined. After developing the program in the Python language, a test with synthetic data was performed as input data. The test was done using a binary image of two sinusoids, a straight line and random noises (Torres et al., 1990). The composition of the image was made in such a way as to simulate all the possible features that an image log may have (results not shown in this article). After validating the program for synthetic data, it was used to treat a real data found in Zhang & Xiao, (2009), which is an example of a resistive image log.

Results

In this section, we present only the validation of the proposed method in a real resistive image log. Figure 3a shows the original resistive log published by Zhang and Xiao (2009) in depth. As mentioned in the methodology, a pre-processing was done in the original data so that it could serve as input data for the program. After this, a dithering of the original image was performed, shown in Figure 3b. Dithering is a technique that consists of overlapping two images with different colors to give the impression that it is just an image, simulating a third color through the mentioned overlap (Moraes, 2013).

After preprocessing the image, we use this as input data for the program. The image has dimensions of 244 X 612 pixels, which gives us, according to Equation 1, 459 transformed planes. As the results for a real data are much more complex, the analysis was done using the transformed Hough plane in conjunction with the same already binarized after the cutoff point. In this case, the pixel intensity of 190 was chosen as the cutoff point, which allowed non-sinusoid data to appear in the binary transformed plane, but ensured that no sinusoids were lost. And so, a histogram for the real image was generated, which is not shown in this article (Moraes, 2013).

Thus, by analyzing the Hough transformed and the transformed binarized planes, we arrive at eight possible senoids, which were numbered according to their depth of reference. The smallest depths are for the sine waves at the top of the input image. For example, sine number one has a phase of 244 °, an amplitude of 31 pixels and is centered at a depth of 107 pixels. This analysis was performed for each of the 8 senoids (Figure 4). Comparing the results obtained in the present work with the results obtained by Zhang and Xiao (2009), it can be seen that there is a similarity between the results. The number of senoids found by the program was the same as found by Zhang and Xiao (2009), and the geologist's analysis found fewer flaws in the log. Figure 4 shows the results obtained by Zhang and Xiao (2009), the analysis done by the geologist and the graph made with the senoids that the program found (Moraes, 2013).

Conclusions

In the present work, HT was used as the main tool in the semi - automatic identification of fractures in real resistive image logs found in the literature. To achieve these objectives, we developed a program in the Python language and to validate the methodology, the results were compared with those published by Zhang and Xiao (2009). The number of fractures found was the same found in this publication, with amplitudes ranging from 26 to 59 pixels, while the phase ranged from 68° to 300°. The processing time was 40 seconds per analyzed image line, each line with 212 pixels. Finally, comparing the results obtained with the analysis and interpretation done by a geologist, it can be said that the approach adopted in this work is appropriate in the analysis of resistive image logs.

Acknowledgments

We thank UENF/LENEP for the computational infrastructure.

References

- AlbinHassan, M. & Marfurt, K. 2003, Fault detection using Hough transforms: 73rd Annual International Meeting, SEG, Expanded Abstracts, 1719–1721.
- Duda, R. & HART, P. 1972. Use of the Hough transformation to detect lines and curves in pictures. *Communications of the ACM*, ACM, v. 15, n. 1, p. 11–15.
- Ellis, D. & Singer, J. 2007. *Well logging for earth scientists*. Springer Verlag, The Netherlands, 708 p.
- Glossop, K.; Lisboa, P.; Russell, P.; Siddans, A. & Jones, G. 1999. An implementation of the Hough transformation for the identification and labelling of fixed period sinusoidal curves. *Computer Vision and Image Understanding*, Elsevier, v. 74, n. 1, p. 96–100.
- Gonzalez, R. & Woods, R. 2002. *Digital Image Processing*. Digital Image Processing, Prentice Hall, Upper Saddle River, 528 p.
- Hough, P; 1962. Method and means for recognizing complex patterns, U.S. Patent 3069654.
- Jain, A. 1989. *Fundamentals of Digital Image Processing*. Prentice-Hall, Upper Saddle River, 569 p.
- Moraes, C. 2013. Use of the Hough Transform to identify fractures in resistive image logs. *Course Completion Work, UENF - Macaé*, 87 p. (In Portuguese).
- Prenskey, S. 1999. *Advances in borehole imaging technology and applications*. Geological Society, London, Special Publications, Geological Society of London, v. 159, n. 1, p. 1–43.
- Thapa, B.; Hughett, P. & Karasaki, K. 1997. Semi-automatic analysis of rock fracture orientations from borehole wall images. *Geophysics, Society of Exploration Geophysicists*, v. 62, n. 1, p. 129–137.
- Torres, D.; Strickland, R. & Gianzero, M. 1990. A new approach to determining dip and strike using borehole images. *Halliburton Rept*, p. 1–7.
- Zhang, X. & Xiao, X. 2009. Detection of fractures in borehole image. *International Society for Optics and Photonics. Sixth International Symposium on Multispectral Image Processing and Pattern Recognition*. p. 749541–749541.

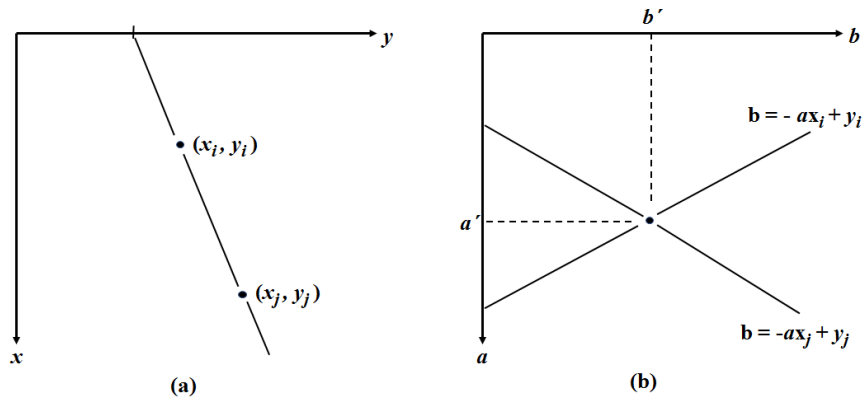


Figure 1. (a) Normal and (b) transformed plane (modified by Gonzalez & Woods, 2000).

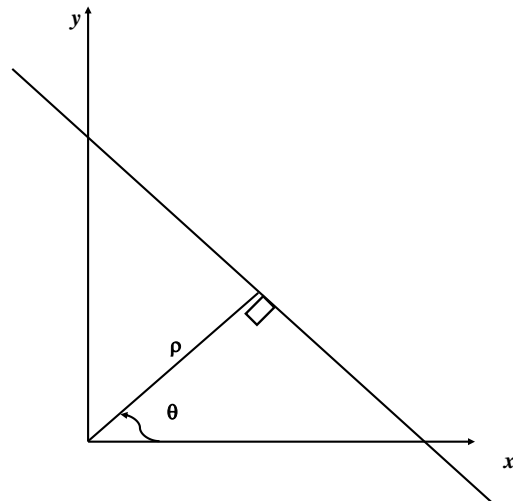
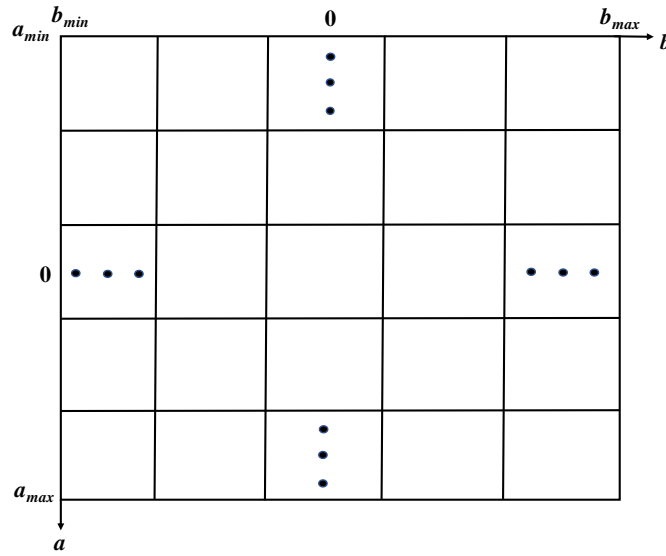


Figure 3. Normal representation of a line (modified by Duda & Hart, 1972).

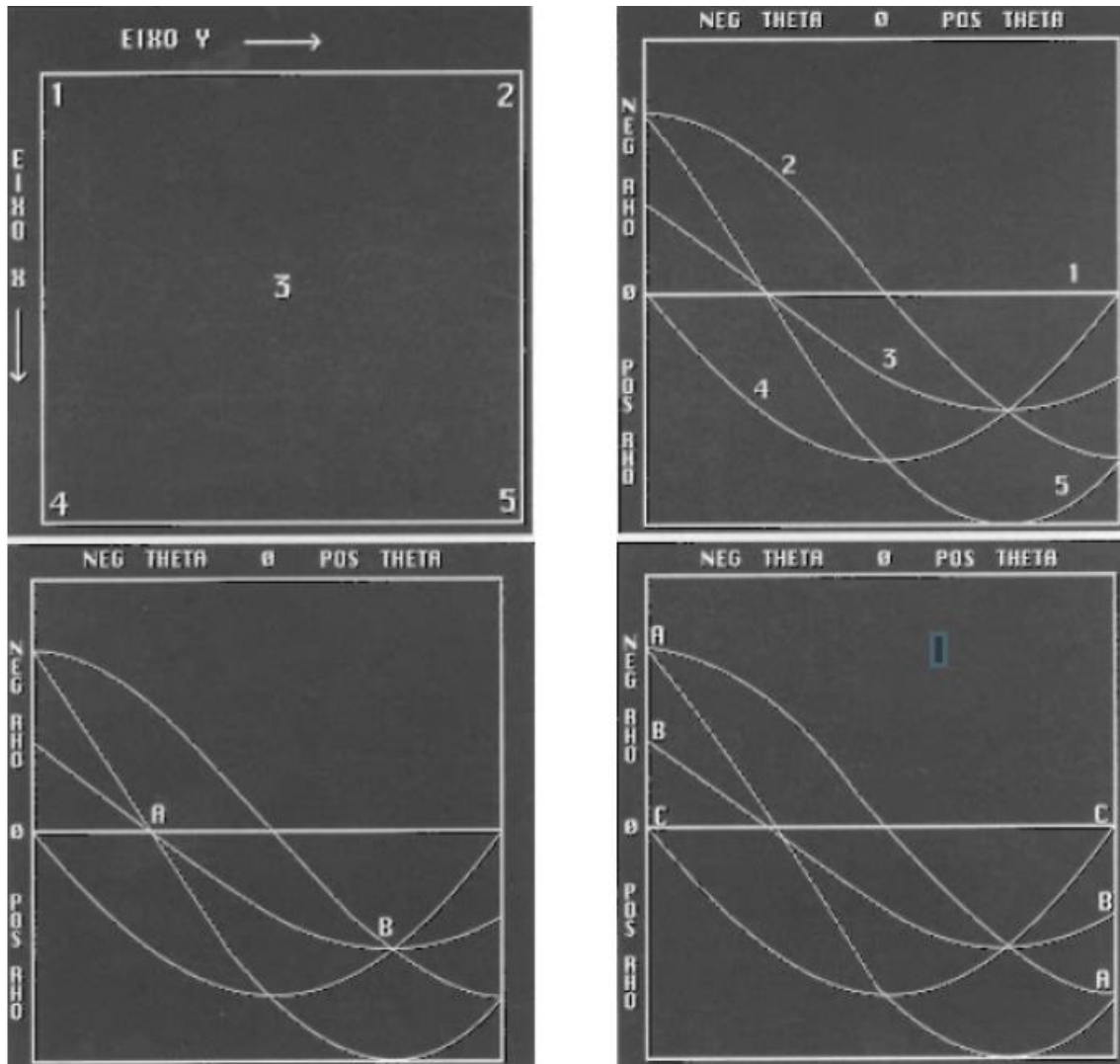


Figure 4. Example of the Hough Transform (modified by Gonzalez & Woods, 2000).

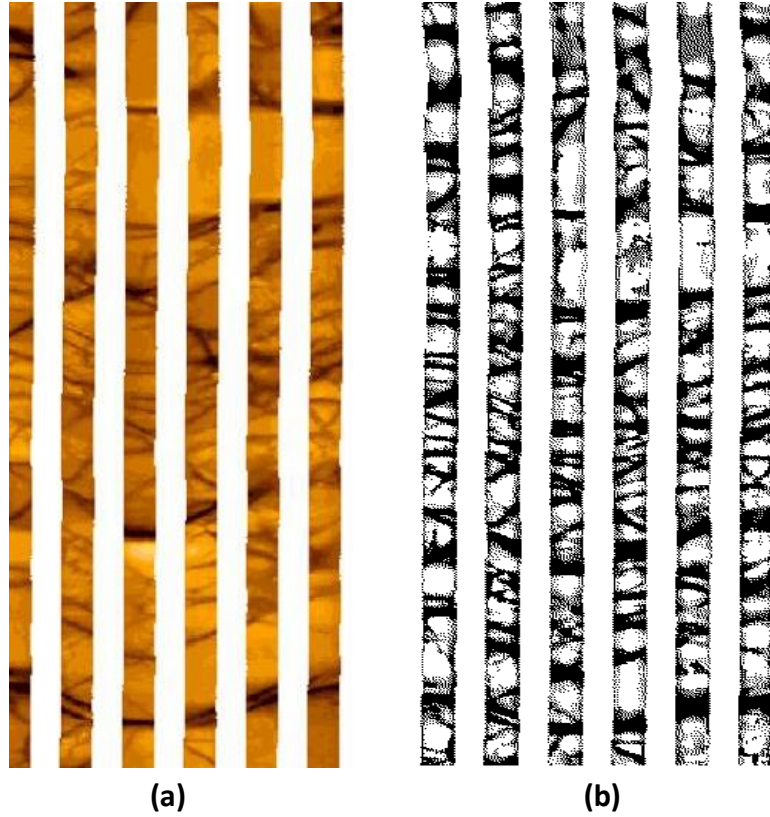


Figure 5. (a) Resistive image log used to validate the methodology (modified by Zhang & Xiao, 2009). (b) Image after pre-processing in our work.

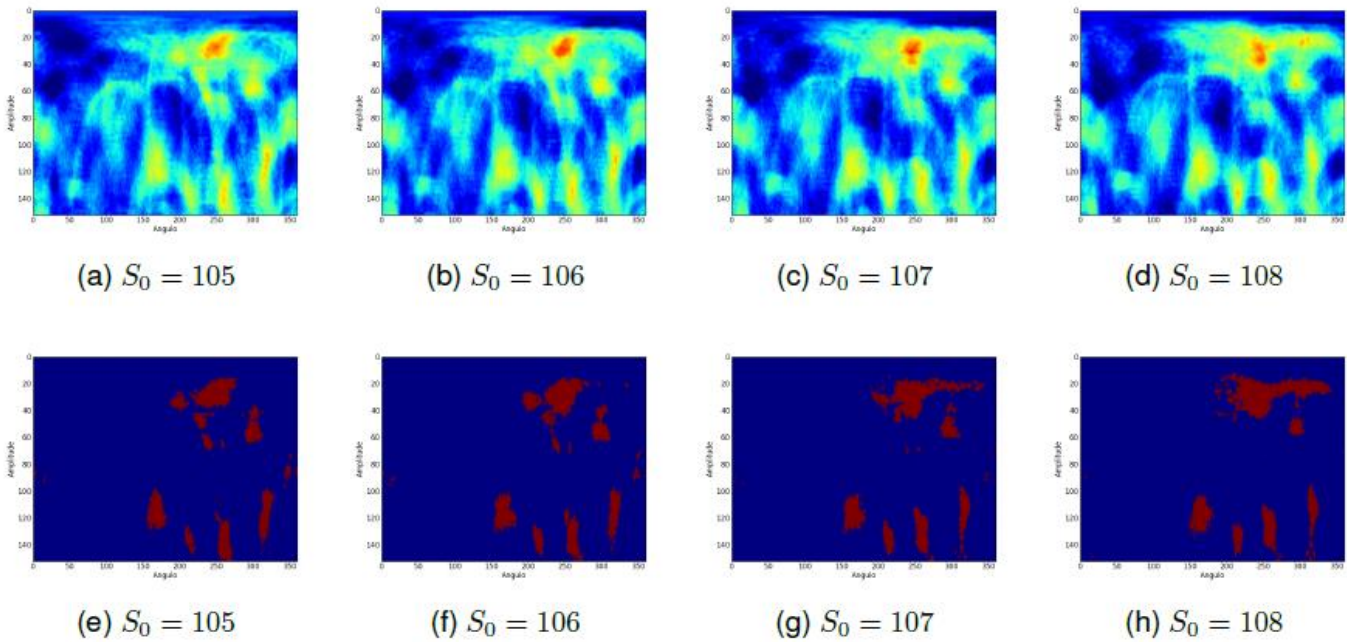


Figure 6. Plans transformed from Hough to the sine one . Figures (a) to (d) are the colored planes, and (e) to (h) are the binarized planes.

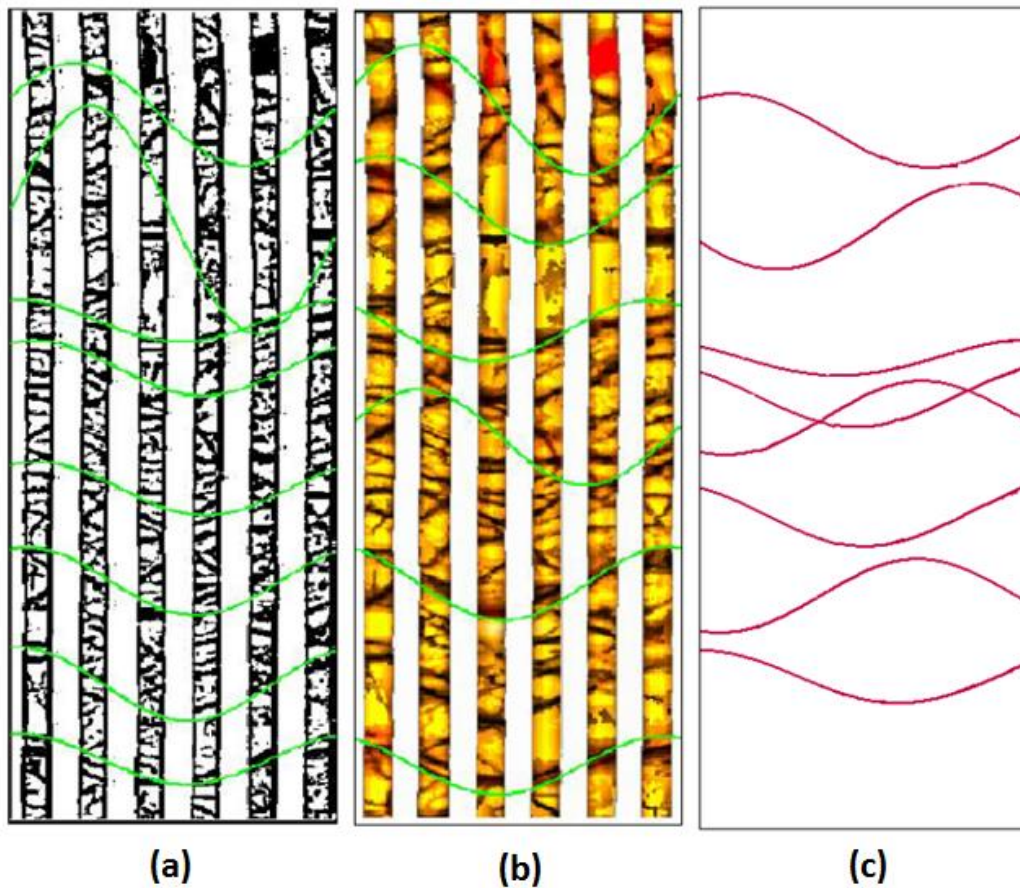


Figure 7. (A) Result obtained by Zhang and Xiao (2009). (B) Analysis of the geologist published in the work of Zhang and Xiao (2009). (C) Result obtained by the software developed in the work.